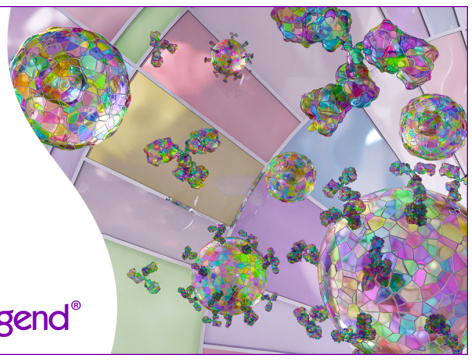

The Journal of Immunology
RESEARCH ARTICLE | MARCH 22 2023

A Therapeutic Vaccine in Combination with Cyclic GMP–AMP Cures More Differentiated Melanomas in Mice

Md Masud Alam; ... et. al

J Immunol (2023) 210 (9): 1428–1436.
https://doi.org/10.4049/jimmunol.2200371

Related Content

Therapeutic Vaccine (TheraVac) in combination with cGAMP cures more differentiated melanomas in mice
J Immunol (May,2021)

Development of a curative therapeutic vaccine (TheraVac) for the treatment of large established tumors
J Immunol (May,2017)

Development of a Curative Immunotherapeutic Strategy for the Treatment of Big Established CT26 Tumors
J Immunol (May,2016)

A Therapeutic Vaccine in Combination with Cyclic GMP–AMP Cures More Differentiated Melanomas in Mice

Md Masud Alam,* Timothy Gower,† Mengmeng Jiang,* Joost J. Oppenheim,*,[1] and De Yang*

We have identified a combinational immunotherapy termed TheraVac vaccine (TheraVac) that can cure multiple large established mouse tumors, but it failed to cure melanoma in mice. TheraVac consists of an immunostimulating arm containing an agonist (HMGN1 [N1]) for TLR4 and an agonist (R848) for TLR7/8 that synergize to activate tumor-infiltrating dendritic cells (DCs) and promote Th1 immune responses. The second arm uses an immune checkpoint blockade, anti-PDL-1, to diminish tumor-associated immunosuppression. In this study, we investigated supplementation of TheraVac by a stimulator of IFN genes (STING) agonist, cyclic GMP–AMP (cGAMP), because together they synergize in activating DCs and produced more immunostimulating IL-12p70 and TNF-α cytokines. The synergistic activation and maturation of DCs is dependent on the activation of tank binding kinase-1 (TBK1). Treatment of three different melanin-producing mouse melanomas (B16F1, M3, and M4) with intratumoral delivery of cGAMP and TheraVac eradicated 60–80% of these melanomas. Immunoprofiling of M3 tumor treated with TheraVac plus cGAMP showed an increase in $CD8^+$ CTLs and macrophages in the tumor. There was also a marked increase of CD4, CD8 effector and memory T cells and generation of functional tumor-specific CTLs in tumor-draining lymph nodes. The resultant tumor-free mice were selectively resistant to subsequent challenge with the same tumors, indicating long-term tumor-specific protective immunity. Overall, our findings have important implications for clinical trials with a combination of these immunotherapeutics to cure melanin-producing human melanomas, without the need for exogenous tumor Ags and no clear toxic effects in mice. ***The Journal of Immunology*****, 2023, 210: 1428–1436.**

Melanoma is a type of skin cancer originating from transformed melanocytes. Advanced metastatic melanoma is invariably fatal and presents a median survival of 6 mo, and a 5-y survival rate of <5% (1). Clinically, cutaneous melanomas are difficult to treat, and surgical resection is the best option for patients with localized disease, but it is not effective for the patients with regional metastasis. Targeted therapies using inhibitors for certain signal transduction pathways, such as BRAF/MEK inhibitors, MEK inhibitors, and MEK/PI3K/AKT/mTOR inhibitors, result in a partial response in overall survival in melanoma patients, but only for a short duration because of the development of resistance to these therapies (2–5). Immunotherapy using cytokines or checkpoint blockade, including the gp100 peptide vaccine, a high dose of IL-2, or anti-CTLA4 mAb (ipilimumab), shows a clinical benefit for only 10–30% of patients (6–9). Furthermore, only a minority of these patients display a long-lasting clinical response and develop systemic $CD8^+$ T cell responses specific for defined melanoma Ags, suggesting that additional barriers might need to be overcome to maximize therapeutic efficacy. The most efficacious treatment for advanced melanoma today is combination immunotherapy of anti-PD-1 and anti-CTLA4, with response rates >50% (10–12). However, such combination immunotherapy has severe toxicity, and most melanoma patients treated with such combination eventually develop resistance, necessitating the development of additional safe and novel treatments.

We have developed an immunotherapeutic regimen termed "therapeutic vaccine (TheraVac)" that consists of agonists for TLR4 (HMGN1 [N1]) and TLR7/8 (R848) that synergize to activate tumor-infiltrating dendritic cells (TiDCs) and upregulate Th1 immune responses, along with a checkpoint inhibitor (anti-PDL-1) to diminish tumor-associated immunosuppression. TheraVac can cure a number of established large mouse tumors, but it fails to cure melanoma in mice (13–15). We investigated numerous supplements to boost the TheraVac regimen and identified that cyclic GMP–AMP (cGAMP), a stimulant of the stimulator of IFN genes (STING) pathway (16, 17), when added to the immunostimulatory arm of TheraVac synergistically induces DC maturation and production of the immunopromoting IL-12p70 and TNF-α cytokines. We also determined whether the combination of TheraVac and cGAMP could effectively treat various mouse melanomas, including poorly immunogenic B16F1 (18–20), a carcinogen-induced melanocytic melanoma (M3), and a transitory melanoma with a RAS mutation (M4) (21). The results show that mice bearing these differentiated melanomas were cured when treated with

*Cellular Immunology Section, Cancer Innovation Laboratory, Center for Cancer Research, National Cancer Institute, Frederick, MD; and †Frederick National Laboratory for Cancer Research, Frederick, MD

[1]Deceased.

ORCIDs: 0000-0001-5611-921X (T.G.); 0000-0002-9069-0150 (M.J.); 0000-0001-6705-8504 (D.Y.).

Received for publication May 26, 2022. Accepted for publication February 22, 2023.

This work was supported in part by the Intramural Research Program of National Institutes of Health through National Cancer Institute Grant HHSN261200800001E. The content of this publication does not necessarily reflect the views or policies of the Department of Health and Human Services, nor does mention of trade names, commercial products, or organizations imply endorsement by the U.S. Government. This research was supported in part by the Intramural Research Program of that National Institute of Health, Frederick National Lab, Center for Cancer Research. The publisher or recipient acknowledges right of the U.S. Government to retain a nonexclusive, royalty-free license in and to any copyright covering the article.

M.M.A. and D.Y. conceived and designed the study; M.M.A., T.G., and D.Y developed methodologies and provided data acquisition; M.M.A., D.Y., and J.J.O. analyzed and interpreted data and wrote the manuscript; M.M.A. and D.Y. reviewed and/or revised the manuscript; M.J. provided experimental and technical support; and D.Y. supervised the study.

Address correspondence and reprint requests to Dr. Md Masud Alam and Dr. De Yang, Cellular Immunology Section, Cancer Innovation Laboratory, Center for Cancer Research, National Cancer Institute, Building 560/Room 31-19, 1050 Boyles Street, Frederick, MD 21702-1201. E-mail addresses: md.alam@nih.gov (M.M.A.) and yangd@mail.nih.gov (D.Y.)

The online version of this article contains supplemental material.

Abbreviations used in this article: BMDM, bone marrow–derived macrophage; cGAMP, cyclic GMP–AMP; DC, dendritic cell; dLN, draining lymph node; h, human; HPC, hematopoietic progenitor cell; LLC, Lewis lung carcinoma; m, mouse; MoDC, monocyte-derived DC; N1, HMGN1; NCI, National Cancer Institute; STING, stimulator of IFN genes; TBK1, TANK-binding kinase-1; TdR, thymidine deoxyribose; TheraVac, therapeutic vaccine; TiDC, tumor-infiltrating DC; TME, tumor microenvironment.

the combination of TheraVac and cGAMP. The tumor-free mice were resistant to subsequent rechallenge with the same melanomas, but not unrelated tumors, indicative of persistent long-term tumor-specific immunity. Mechanistically, the immunostimulatory arm of TheraVac plus cGAMP synergistically stimulated the activation/maturation of DCs through cooperative activation of TANK-binding kinase-1 (TBK1), a kinase critical for DC production of cytokines including IFNs. In comparison with M3-bearing mice treated with TheraVac, M3-bearing mice treated with the combination of TheraVac and cGAMP manifested more robust antitumor immune responses. Thus, treatment with the combination of TheraVac and cGAMP induced effective antitumor responses in M3-bearing mice without exogenous tumor Ags. Because these melanomas are homologous with human melanomas at respective stages, these results may be relevant for potential clinical application.

Materials and Methods

Cell lines, mice, and reagents

The cell line B16F1 used in the current study was initially purchased from the American Type Culture Collection (Manassas, VA). CL-3 for M3 and CL-4 for M4 melanin- producing melanoma cell lines were obtained from Dr. Glenn Merlino's laboratory at National Cancer Institute (NCI)/National Institutes of Health (Bethesda, MD) (21). C57BL/6Ncr (8- to 12-wk-old, female) mice were provided by the animal production facility of the NCI. C57BL/6J (8- to 12-wk-old, female) mice were purchased from The Jackson Laboratory. All experiments with mice were performed in compliance with the principles and procedures outlined in the National Institutes of Health *Guide for the Humane Care and Use of Animals* and were approved by the NCI at Frederick Animal Care and Use Committee. Recombinant N1 was produced in-house using *Escherichia coli* expression system as previously reported (15). R848, BX795, and 2′3′-cGAMP were obtained from InvivoGen. Anti-PDL-1 (clone 10F.9G2) was purchased from Bio X Cell (Lebanon, HN). Collagenase I, collagenase II, collagenase VI, DNase I, and elastase were purchased from Worthington Biochemical (Lakewood, NJ).

Isolation and purification of primary immune cells

Human peripheral blood samples were obtained from healthy donors (Transfusion Medicine Department, Clinical Center, National Institutes of Health, with an approved human subject agreement) by leukapheresis (13, 22). PBMCs were isolated by Ficoll-Hypaque density gradient centrifugation (23). Monocytes and $CD4^+$ T cells were purified (>95%) from PBMCs with the use of MACS cells isolation kits (Miltenyi Biotec) according to the manufacturer's instructions. Mouse bone marrow–derived cells were collected from the C57BL/6Ncr (NCI–Frederick, National Institutes of Health). Mouse bone marrow–derived hematopoietic progenitor cells (HPCs) were prepared by flushing from femur and tibia with the depletion of RBCs by ammonium chloride treatment (24).

Generation and stimulation of DCs and macrophages

Human monocyte-derived DCs (MoDCs) were generated by culturing purified monocytes at 5×10^5/ml in complete RPMI 1640 medium (RPMI 1640 medium supplemented with 10% FBS, 2 mM glutamine, 25 mM HEPES, 100 U/ml penicillin, 100 μg/ml streptomycin, and 50 μM 2-ME) containing 50 ng/ml human (h)GM-CSF and 50 ng/ml hIL-4 at 37°C in a humidified CO_2 (5%) incubator for 5 d with 50% of the culture medium replaced with prewarmed fresh complete RPMI 1640 medium containing hGM-CSF and hIL-4 at the same concentration on 3 d. On day 5 of culture, DC suspensions were harvested as immature DCs and used for the subsequent experiments. Mouse bone marrow–derived DCs (BMDCs) were generated by culturing mouse HPCs isolated from the femurs and tibias in complete RPMI 1640 containing 20 ng/ml mouse (m)GM-CSF for 6 d. On days 2 and 4 of culture, nonadherent cells were removed by mild pipetting and the remaining adherent cells were cultured in the complete medium containing mGM-CSF at the same concentration as indicated above (25). On day 6 of culture, DC suspensions were harvested as immature DCs and used for the subsequent experiments. For BMDM or monocyte-derived macrophage generation, HPCs (1×10^6/ml) or monocytes (1×10^6/ml) were cultured for 6 d in complete RPMI 1640 medium in the presence of 50 ng/ml mM-CSF or hM-CSF with 50% replacement of the cultured medium on day 3. On day 6–7 of the culture, macrophages were harvested for the treatment with one or more of the following stimulators (e.g., N1, R848, cGAMP) for the indicated periods of time at 37°C in a CO_2 incubator before being analyzed for phenotype, function, and signaling.

Allogeneic MLR

MLR was performed as reported previously (13). Briefly, human MoDCs were treated with N1 (0.62 μg/ml), R848 (0.62 μg/ml), or cGAMP (0.5 μg/ml) alone or in combination for 24 h. The treated MoDCs were cocultured with allogeneic $CD4^+$ T cells at the ratio of $CD4^+$ T cells/MoDCs of 30:1 in triplicate in a 96-well plate for 4 d. The cultures were pulsed with [^{3}H]-thymidine deoxyribose (TdR) (0.5 mCi/well, New England Nuclear) for the last 12 h before being harvested for the measurement of [^{3}H]-TdR incorporation using a MicroBeta counter (Wallac, Gaithersburg, MD). Alternatively, the supernatants of cocultures of $CD4^+$ T cells/treated MoDCs at a ratio of 50:1 for 3 d were collected for cytokine quantitation. The data were analyzed by GraphPad Prism version 7.

Quantitation of cytokines

Multiple cytokines in the culture supernatants of human and mouse DCs or in the supernatants of MLR were measured using V-PLEX ultrasensitive plate assays (Meso Scale Discover) (13). The plates were analyzed using an MSD Sector image 2400 (Meso Scale Discovery) according to the manufacturer's protocol. The data comparing the means of the treated samples to those of the untreated control were analyzed by GraphPad Prism (version 8.4.3).

Western blot analysis

Western blots were performed as described previously (13). Briefly, human MoDCs starved in serum-free medium containing 50 ng/ml hGM-CSF and 50 ng/ml hIL-4 at 37°C in a humidified CO_2 (5%) incubator were incubated with N1, R848, and cGAMP by themselves or all together for a period as specified. The treated and untreated cells were lysed in SDS whole-cell lysis buffer at 10^7/ml for 30 min at room temperature. The samples were boiled for 5 min, cooled on ice, loaded (15 μl/lane for whole-cell lysates), and separated on a 4–12% NuPAGE Bis-Tris gel using 1× NuPAGE MOPS SDS running buffer as the electrode buffer. SeeBlue Plus2 was used as a molecular size marker. After transfer of separated proteins onto polyvinylidene difluoride membranes, the membrane was blocked with blocking buffer (1× TBST containing 5% nonfat milk) at room temperature for 1 h and incubated overnight at 4°C with Abs (1:1000 diluted in blocking buffer) against p-TBK1 (D52C2, S172) as the first Ab. After washing with TBST, the membranes were reacted with HRP-conjugated goat anti-rabbit IgG (7074S) as the secondary Ab (1:2000 diluted in blocking buffer) and then washed and developed in the SuperSignal West Dura extended duration substrate. The images were collected using the G:BOX Chemi systems. Subsequently, the same membrane was stripped by blot stripping buffer and probed consecutively in the same manner using TBK1 (D1B4) and GAPDH (14C10) as the first Abs.

Mouse tumor model and treatment

Female mice (C57BL/6, $n = 5$, 8–12 wk old) were s.c. injected with 0.1 ml of PBS containing B16F1 (2×10^6/ml), M3 (2×10^6/ml), or M4 (2×10^7/ml) melanomas into their right flank regions. Mice bearing melanoma tumors of ~0.7 cm in diameter were intratumorally treated with anti-PDL-1 (10 μg/injection), N1 (10 μg/injection), R848 (10 μg/injection), and cGAMP (5 μg/injection) alone or in combination as specified. The appearance and size of tumors were monitored twice weekly. Tumor sizes were calculated using the formula $(L \times W^2)/2$, where the length (L) and width (W) of the tumors were measured with a caliper. The survival curve was generated using a Kaplan–Meier plot. The cured tumor-free mice were kept for 65–75 d and rechallenged with same types of melanoma cells onto the right flank and different unrelated tumors cells on the contralateral left flank. The formation and growth of tumors were monitored for ~3 wk.

RNA extraction, cDNA synthesis, and real-time PCR

Melanoma tumors with or without treatment were resected and followed the instructions of the TRIzol reagent manufacturer for isolation of total RNAs. The RNA was purified using an RNeasy micro kit with on-column DNase digestion to eliminate possible genomic DNA contamination. Purified RNA (500 ng) was reverse transcribed to cDNA with a QuantiTect reverse transcription kit. Twenty nanograms of cDNA was used for quantitative real-time PCRs. Quantitative real-time PCRs were performed with an RT^2 DNA SYBR Green ROX kit on a LightCycler 480 II RT-PCR (Roche) system to measure the expression of human and mouse cytokines using specific primers obtained from Qiagen. ΔCt values were obtained by deducting the raw cycle threshold (Ct values) obtained from mouse β-actin mRNA (Qiagen, PPM02945B-200), the internal standard, from the Ct values obtained for investigated mouse IFN-β (Qiagen, PPM03594C), IFN-γ (Qiagen, PPM03121A-200), CXCL9 (Qiagen, PPM02973B-200), and CXCL10 (Qiagen, PPM02978E-200) genes. For graphical representation, data are expressed as fold mRNA level increase compared with the expression level in unstimulated cells using GraphPad Prism (version 8.4.3).

Preparation of single-cell suspension of tumor tissue

The tumors were sliced (~1 mm^3) in cold Leibovitz L-15 medium (Thermo Fisher Scientific). These slices were subsequently digested at 37°C for 45 min with constant shaking (85 rpm) in Leibovitz L-15 medium containing collagenase I (0.17 mg/ml), collagenase II (0.056 mg/ml), collagenase VI (0.17 mg/ml), DNase I (0.025 mg/ml), and elastase (0.025 mg/ml). At the end of incubation, the digested samples were immediately kept on ice for 10 min to allow the tissue debris to sediment to the bottom of the tubes. Cell suspension was collected and filtered through a 70-μm nylon cell strainer. Cells in the suspension were then washed and suspended in RPMI 1640 complete medium for downstream analysis.

Immunostaining and flow cytometry

Immunostaining and flow cytometry analysis were done according to the protocol described (13). Briefly, treated and untreated DCs/macrophages were washed with flow cytometry buffer, blocked for 10 min with blocking buffer, and subsequently stained with mAbs against human CD80-PE (R&D Systems, catalog no. FAB140P), CD80-allophycocyanin (BioLegend, clone 2D10, catalog no. 305219), CD83-PE (BD Pharmingen, catalog no. 556855), CD86-FITC (BD Pharmingen, catalog no. 555657), HLA-ABC-PE-Cy7 (BioLegend, clone W6/32, catalog no. 311430), CD14-Pacific Blue (BioLegend, clone M5E2), CD206-FITC (BioLegend, clone 15-2), and CD163-allophycocyanin (BioLegend, clone GHI/61) or mouse CD80-PE-Cy7 (BioLegend, clone 16-10A1), CD86-PerCP-Cy5.5 (BioLegend, clone GL-1), CD11c-allophycocyanin (BD Pharmingen, clone HL3), and I-A/I-E-FITC (BD Pharmingen, clone 2G9) at 4°C for 30 min. The stained cells were washed with flow cytometry buffer once and with PBS twice before analyzing the surface expression molecules on LSR II SORP flow cytometer (BD FACSCalibur).

For melanocytic melanoma tumors, lymph nodes were resected to make a single-cell suspension for the quantification of infiltration immune cells on a FACSymphony A5 flow cytometer. The Abs used to stain the samples were anti-mouse CD45-BB515 (BioLegend, clone 30-F11), CD3-PE-Cy5.5 (Invitrogen, clone 145-2C11), CD4-BV421 (Invitrogen, clone RM4.5), CD4-allophycocyanin-Cy7 (BioLegend, clone GK1.5), CD8-allophycocyanin-Cy7 (Tonbo Biosciences, clone 53-6.7), CD8-PE-Cy7 (Tonbo Biosciences, clone 2.43), CD11c-allophycocyanin (BD Biosciences, clone HL3), CD11b-PE (BD Biosciences, clone M1/70), B220-BV605 (BioLegend, clone RA3-6B2), CD44-Pacific Blue (BioLegend, clone IM7), and CD62L-allophycocyanin (BioLegend, clone MEL14). The stained samples were analyzed and collected on a FACSymphony A5 flow cytometer (BD Biosciences). All flow cytometry data were analyzed using FlowJo software version 10.7.1.

CD107a mobilization assay

Analysis of the mobilization of CD107a on the surface of CTLs specific for melanomas was followed according to the protocol previously described (26). Briefly, draining lymph nodes (dLNs) of the treated and untreated M3 melanoma-bearing mice were removed to make single-cell suspensions. The lymphocytes of the dLNs (1×10^6/ml) were seeded as an effector cell to monolayer M3 (2×10^5/ml) melanomas as target cells in a 48-well plate at an E:T ratio of 5:1. After coculture of the plate for 24 h at 37°C, the lymphocytes were harvested, washed with flow cytometry buffer, blocked with blocking buffer on ice for 10 min, and subsequently stained with anti-mouse CD8a-eFluor 450 (Invitrogen, clone 53-6.7) and anti-CD107a-eFluor 660 (Invitrogen, clone 1D4B) Abs on ice for 30 min. The samples were resuspended in FACS buffer and data were acquired on an LSR II flow cytometer. Lymphocytes incubated without M3 cells served as a negative control.

Quantification and statistical analysis

Statistical significance between control and treated datasets was determined by a Student *t* test. A repeated or one-way ANOVA, followed by a Tukey's post hoc test, was applied to identify the statistical significance in datasets with more than two groups. The log-rank test was used to analyze the survival difference in treatment and control mice. A p value of <0.05 was considered significant. All error bars represent the mean ± SD.

Results

STING activation by cGAMP boosts the DC-activating effect of the immunostimulatory arm of TheraVac

Because the immunostimulatory arm (N1 and R848) of TheraVac synergically activated and maturated DCs, but failed to cure resistant melanomas when combined with a checkpoint inhibitor (13, 15), we therefore screened a number of reagents that would boost the activation of DCs and potentially cure mouse melanomas. Indeed, we have identified a STING agonist cGAMP that cooperatively boosted the expression of surface CD80, CD83, CD86, and HLA-ABC on human MoDCs (Fig. 1A) and their production of IL-12p70 and TNF-α in a synergistic manner (Fig. 1B, Supplemental Fig. 1) when combined with the immunostimulatory arm of TheraVac.

Based on recent reports characterizing the STING signaling pathway, DC activation appears to be triggered through phosphorylation of TBK1. TBK1 is involved in the activation of both IRF3 and NF-κB triggered by TLR and STING agonists (27, 28). Therefore, we further investigated whether combination of the immunostimulatory arm of TheraVac and cGAMP could cooperatively induce TBK1 phosphorylation in DCs. To this end, TBK1 phosphorylation in MoDCs after treatment with N1, R848, and/or cGAMP was measured by Western blot. Indeed, stimulation by the combination of N1, R848, and cGAMP synergistically induced the phosphorylation of TBK1 in human MoDCs (Fig. 1C, upper and middle panels). BX795, a potent inhibitor of TBK1 (29), greatly reduced the levels of surface expression of costimulatory molecules (CD80, CD83, and CD86) on human MoDCs induced by the treatment with N1, R848, and cGAMP, indicating that DC maturation/activation induced by N1, R848, and cGAMP was likely mediated by TBK1 signaling (Fig. 1C, lower panel).

To determine whether combination of the immunostimulatory arm of TheraVac and cGAMP would promote functional maturation of DCs, human MoDCs treated with N1, R848, and cGAMP were cocultured with allogeneic human $CD4^+$ T cells in an MLR setting. MoDCs treated with N1, R848, and cGAMP exhibited an elevated capacity to stimulate proliferation of allogeneic CD4 T cells (Fig. 1D) as well as an elevated production of IFN-γ, but not IL-13 or IL-17A (data not shown) (Fig. 1E), suggesting that this combination promoted functional maturation of DCs and enabled DCs to promote differentiation of $CD4^+$ T cells into Th1 cells.

N1 treatment of human monocyte-derived macrophages polarized them into proinflammatory M1 macrophages (Supplemental Fig. 2). Because both STING agonist and R848 are reported to trigger M2 to M1 conversion of macrophages (30–32), the combination of N1, R848, and cGAMP may also promote M1 polarization of macrophages. Indeed, treatment of mouse BMDMs with the combination of N1, R848, and cGAMP markedly induced their production of TNF-α, a cytokine indicative of M1 polarization of macrophages (Supplemental Fig. 3).

Furthermore, when treated with N1, R848, or cGAMP alone or altogether, mouse BMDCs also markedly upregulated expression of costimulatory (CD80, CD86) and MHC class II (I-A/I-E) molecules on their surface (Fig. 1F) and elevated the production of TNF-α (Fig. 1G). These data indicate that cGAMP synergistically boosted the immunostimulatory arm of TheraVac for the activation of APCs, presumably via TBK1.

Antitumor effect of TheraVac plus cGAMP on poorly immunogenic B16F1 melanoma in mice

We were encouraged by the synergy observed in the stimulatory arm of TheraVac and cGAMP regarding DC activation and therefore explored treatment by these reagents together with checkpoint (anti-PDL-1) blockade. We first evaluated the effect of this combination of therapeutics on s.c. B16F1 melanoma, a mouse model for human melanoma characterized as a nonimmunogenic or low-immunogenic tumor, which can readily metastasize from a primary s.c. site to the lungs and form nodules there (19, 20). Intratumoral injection of TheraVac plus cGAMP induced robust tumor regression and durable cures in 80% of the mice bearing B16F1 tumors, whereas cGAMP or TheraVac by themselves elicited only transient therapeutic responses and failed to cure the tumors (Fig. 2A). The 80% cured mice resulting from treatment with a combination of TheraVac and cGAMP survived long term (Fig. 2B) and rejected a re-rechallenge

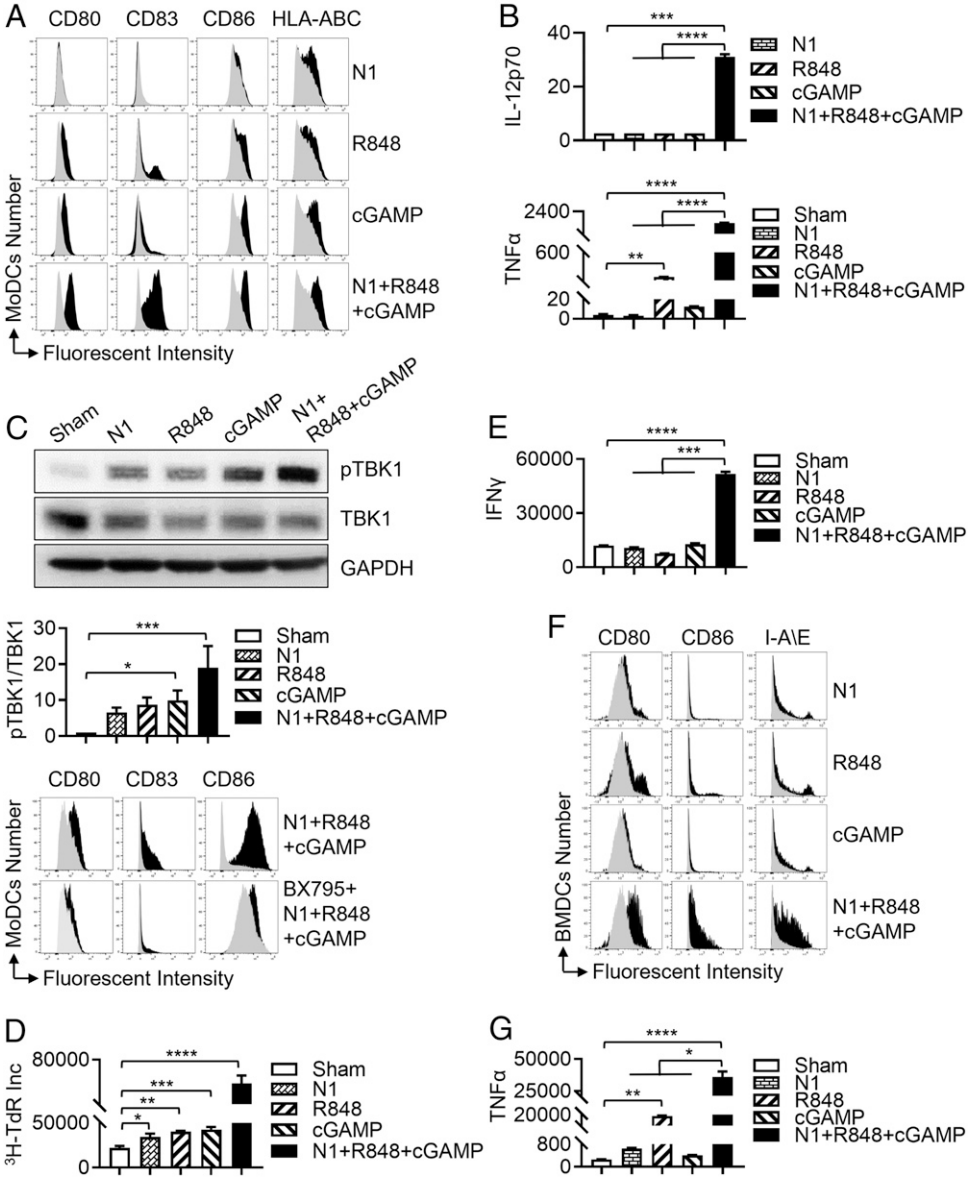

FIGURE 1. N1, R848, and cGAMP synergistically induce phenotypic and functional maturation of DCs. (**A** and **B**) Human MoDCs at 5×10^5/ml were stimulated with N1 (0.25 μg/ml), R848 (0.25 μg/ml), or cGAMP (10 μg/ml) by themselves or all together to determine the effect on expression of surface costimulatory (CD80, CD83, CD86) and HLA-ABC molecules (A) (gray area indicates sham, black area indicates treated), as well as DC production of TNF-α and IL-12p70 (mean ± SD; $n = 3$) cytokines (pg/ml) at 24 h (B). Shown are the results of one experiment representative of three. (**C**) Serum-starved human MoDCs were treated for 90 min with 0.25 μg/ml N1, 0.25 μg/ml R848, or 10 μg/ml cGAMP or altogether before they were solubilized in lysis buffer (0.1 ml) to obtain whole-cell lysates. Identical amounts of whole-cell lysates were loaded onto SDS-PAGE gel and separated by electrophoresis to detect the levels of p-TBK1. After stripping, the membranes were reprobed with TBK1 and/or GAPDH Abs (upper panel). The relative abundance of p-TBK1 was quantitated using ImageJ software and normalized against TBK1 and GAPDH (middle panel). Human MoDCs (5×10^5/ml) were preincubated with or without TBK1 inhibitor BX795 (10 μM) for 6 h before stimulation for 24 h with a combination of N1 (0.25 μg/ml), R848 (0.25 μg/ml), and cGAMP (10 μg/ml) to determine the effect of BX795 on expression of surface CD80, CD83, and CD86 (lower panel). Shown are the results of one experiment out of two. (**D**) MoDCs treated with N1 (0.62 μg/ml), R848 (0.62 μg/ml), and cGAMP (0.5 μg/ml) alone or in combination were cocultured with allogeneic $CD4^+$ T cells at the ratio of $CD4^+$ T cells/MoDCs of 30:1 for 4 d and pulsed with [^{3}H]-TdR for the last 12 h. $CD4^+$ T cell proliferation was measured by [^{3}H]-TdR incorporation (Inc). Shown are the results of one experiment representative of three. (**E**) Supernatants of MLR with the ratio of $CD4^+$ T cells/treated MoDCs of 50:1 incubated for 3 d were quantitated for cytokine (pg/ml) production (average [mean ± SD]). Shown are the results of one experiment representative of three. (**F** and **G**) Mouse BMDCs treated for 24 h as indicated were determined for DC expression of indicated surface markers of CD80, CD86, and I-A/I-E (gray area indicates sham treated) or cytokine (pg/ml) production similarly as in (A) and (B). Shown are the results of one experiment representative of two. *$p < 0.05$, **$p < 0.01$, ***$p < 0.001$, ****$p < 0.0001$, between the sham and treated group using one-way ANOVA followed by a Tukey's post hoc test.

with the B16F1 cells, but not rechallenge with unrelated EL4 thymoma cells (Fig. 2C), indicative of the formation of effective immunological memory. Thus, mice cured of B16F1 tumors by treatment with TheraVac plus cGAMP acquired long-term B16F1-specific systemic immunity.

Antitumor effect of TheraVac plus cGAMP on carcinogen-induced melanin-producing melanoma (M3 and M4) in mice

The therapeutic success of TheraVac plus cGAMP on poorly immunogenic B16F1 melanoma led us to evaluate their curative effects on another preclinical melanocytic melanoma, M3 (21). As shown

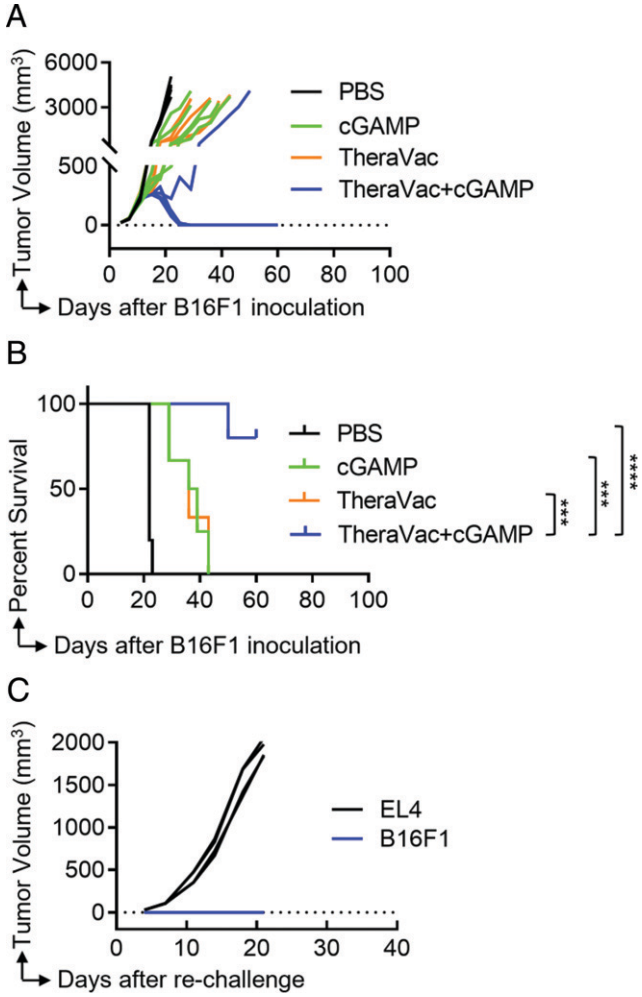

FIGURE 2. TheraVac plus cGAMP cures mice bearing melanin-producing B16F1 melanomas. B16F1 melanoma cells (5×10^5/mouse) were inoculated s.c. into the flanks of C57BL/6 ($n = 5$) mice. On day 8, B16F1-bearing mice were treated by intratumoral injection with PBS, cGAMP, TheraVac, or TheraVac plus cGAMP twice a week for 2 wk. Doses of N1, R848, anti-PDL-1, and cGAMP were 10, 10, 10, and 5 μg/mouse/injection, respectively. (**A** and **B**) The mice were monitored for tumor growth (A) and survival (B) for up to 10 wk. The difference of survival between groups was determined using the log-rank test (***$p < 0.001$, ****$p < 0.0001$). B16F1-free mice (four out of five) were then inoculated s.c. with B16F1 (5×10^5/mouse) cells into the right flank and EL4 (5×10^5/mouse) thymoma cells into the left flank. (**C**) The formation and growth of B16F1 melanoma and EL4 thymoma were monitored and plotted. Shown are the results of one experiment representative of two.

in Fig. 3A, cGAMP or TheraVac by themselves only slightly delayed the growth of M3 tumors, whereas their combination completely eradicated 80% of M3 tumors. Eighty percent of M3-bearing mice treated with cGAMP and TheraVac became long-term tumor-free survivors (Fig. 3B). The mice cured by this treatment were challenged s.c. with M3 cells into the right flank and Lewis lung carcinoma (LLC) cells into the contralateral left flank. (Fig. 3C). The cured mice became specifically resistant to challenge with M3, but not unrelated LLC tumors. This is indicative of development of specific antitumor immunity in the absence of any administered exogenous M3-associated tumor-associated Ags. This quadruple immunotherapeutic combination also cured 60% of slow-growing, low melanin–producing M4 melanomas (data not shown). These data suggest that addition of cGAMP to TheraVac is sufficient for the eradication of melanin-producing melanomas from mice.

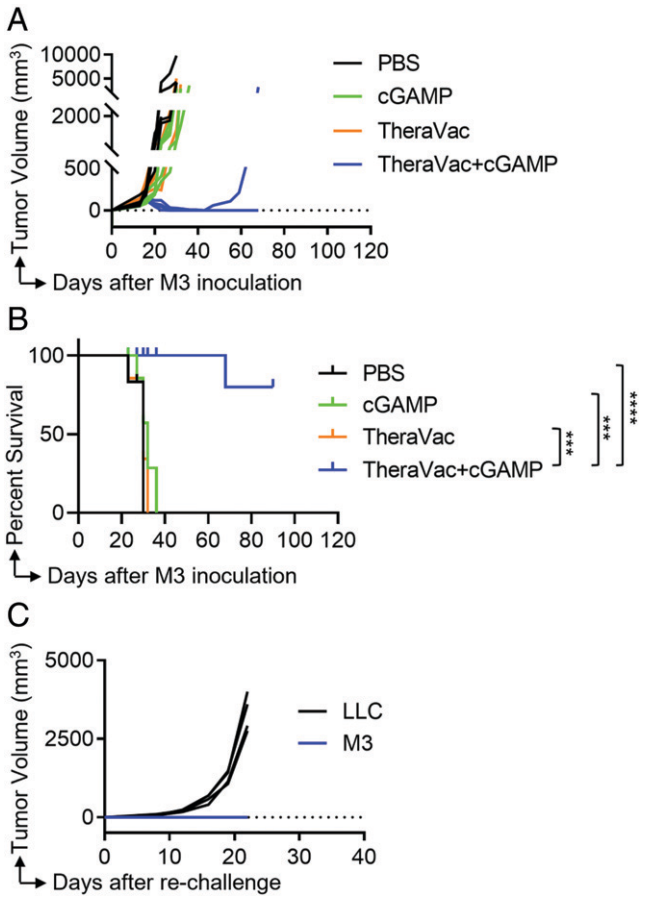

FIGURE 3. TheraVac plus cGAMP cures mice with melanin-producing M3 melanoma. C57BL/6 ($n = 5$) mice were inoculated s.c. with M3 melanoma cells (2×10^5/mouse) into the flanks. On day 13, M3-bearing mice were treated intratumorally with PBS, cGAMP (5 μg/injection), TheraVac (10 μg of each component/injection), or TheraVac plus cGAMP twice a week for 2 wk. (**A** and **B**) The mice were monitored for tumor growth (A) and survival (B) for up to 12 wk. The difference of survival between groups was determined using the log-rank test (***$p < 0.001$, ****$p < 0.0001$). (**C**) M3-free mice (four out of five) were rechallenged s.c. with M3 (2×10^5/mouse) and Lewis lung carcinoma (LLC, 2×10^5/mouse) cells into the contralateral flanks, and the formation and growth of M3 melanoma and LLC carcinoma were monitored and plotted. Shown are the results of one experiment representative of two.

TheraVac and cGAMP combination therapy promotes immune cell infiltration into the melanoma tumors

To understand the mechanisms underlying the observed therapeutic effect of this combination therapy, we analyzed immune responses to TheraVac plus cGAMP therapy in the M3 melanoma model. cGAMP and TheraVac alone moderately increased the infiltration of all leukocytes (Fig. 4A–C, Supplemental Fig. 4). Treatment with a combination of cGAMP and TheraVac markedly increased the infiltration of $CD45^+$ leukocytes (Fig. 4B), $CD4^+$ T, $CD8^+$ T cells, conventional ($CD11c^+B220^-$) DCs, and macrophages ($CD11b^+CD11c^-CD45^+$) (Fig. 4B, 4C), but the infiltration by B ($CD11c^-B220^+$) cells and plasmacytoid ($CD11c^+B220^+$) DCs was similar to the level of the PBS-treated group (Fig. 4B). Quantitative PCR-based quantification of intratumoral cytokines and chemokines revealed that TheraVac plus cGAMP significantly elevated the expression of CXCL9, CXCL10, IFN-β, and IFN-γ, indicating a Th1 signature of the treated tumors (Fig. 4D). CXCL9 and CXCL10 chemokines, critical for the recruitment of Th1 T cells and CTLs to the peripheral tissues, were likely responsible for attracting CD8 CTLs to the

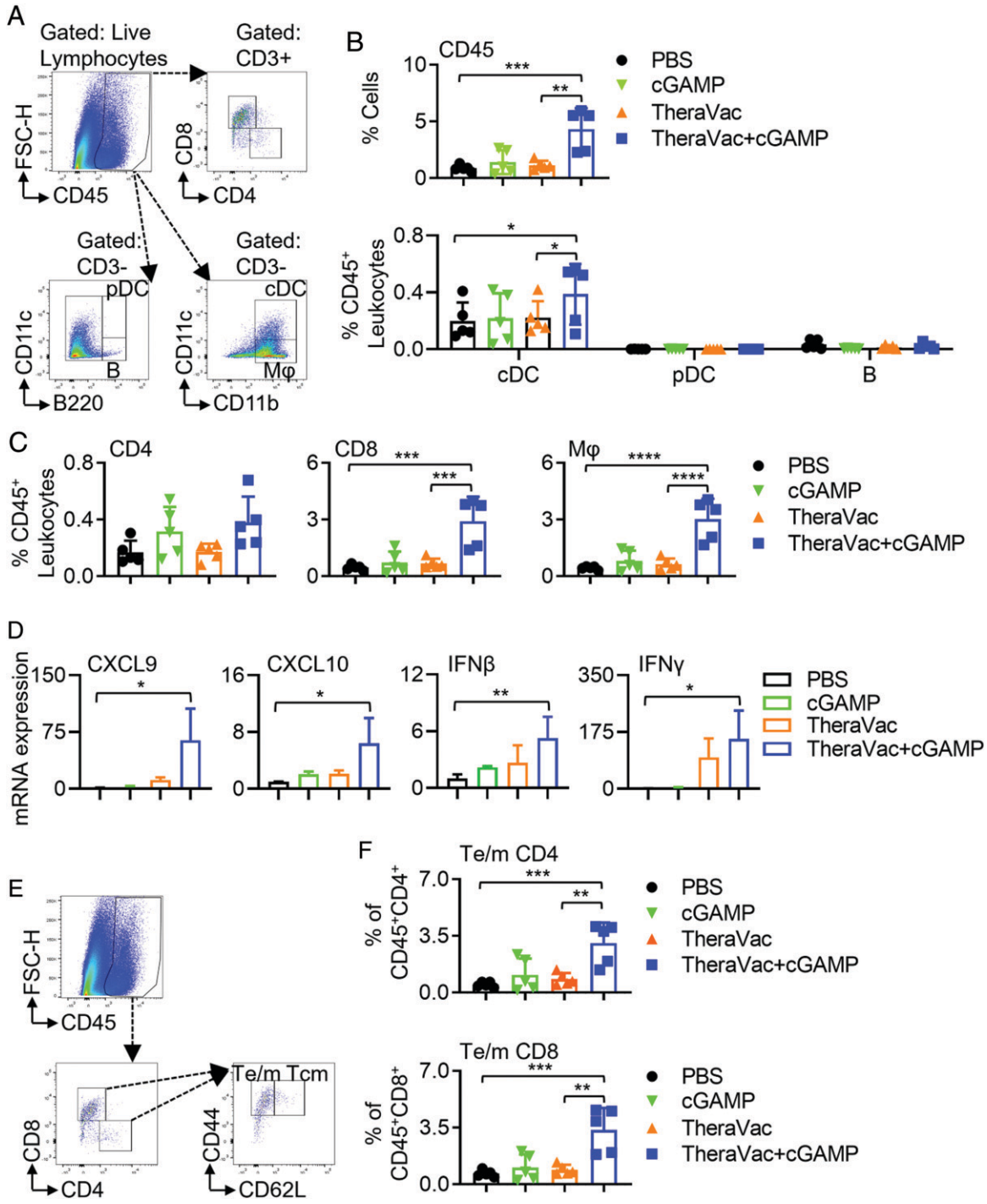

FIGURE 4. Immunoprofiling of M3 tumors treated with TheraVac and cGAMP alone or in combination. C57BL/6 mice inoculated s.c. with M3 melanoma cells (2×10^5/mouse) into the flank were treated on days 13, 16, and 20 with PBS, cGAMP (5 μg/injection), TheraVac (10 μg of each component/injection), or TheraVac plus cGAMP. Twenty-four hours after the last treatment, mice were euthanized to remove the tumors for the preparation of single-cell suspensions for immune staining or for RNA extraction and quantitative PCR analysis. (**A** and **E**) Gating strategy. (**B**–**D** and **F**) Average % (mean ± SD; $n = 5$) of CD45 leukocyte, macrophage (Mφ), plasmacytoid DC (pDC), conventional DC (cDC), B cell, CD4 T, CD8 T, effector/memory (Te/m) ($CD44^{high}/CD62L^{-}$) CD4 T, CD8 T cell infiltration and their expression of CXCL9, CXCL10, IFN-β, and IFN-γ mRNA (fold) in the tumor tissues were measured. Shown are the results of one experiment representative of two. *$p < 0.05$, **$p < 0.01$, ***$p < 0.001$, ****$p < 0.0001$, between the sham and treated group using one-way ANOVA followed by a Tukey's post hoc test.

melanoma tumors. Elevated levels of IFN-γ and IFN-β were indicators of Th1-polarized immune response in melanoma tissue. TheraVac plus cGAMP markedly upregulated the infiltration of effector/memory ($CD44^{high}/CD62L^{-}$) $CD8^{+}$ and $CD4^{+}$ T cells into the melanoma tumor microenvironment (TME; Fig. 4E, 4F, Supplemental Fig. 4). Therefore, the curative effect of TheraVac plus cGAMP on these melanomas was accompanied by, at least in part, augmented infiltration of macrophages and T cells, particularly CTLs and effector/memory CD4, CD8 T cells, and production of factors indicative of Th1-polarized immune responses, such as IFN-β, IFN-γ, CXCL9, and CXCL10, in the tumor tissues.

TheraVac and cGAMP treatment elevated the generation of effector/memory and central memory CD4, CD8 T cells in dLNs of M3 melanoma-bearing mice

Given the DC-activating effects of the immunostimulating arm of TheraVac and cGAMP (Fig. 1), DCs in the TME might be triggered to mature and migrate to the dLNs where they present Ag to T cells for an effective antitumor immune response as previously shown (15). To determine the effective enhancement of effector and memory T cells in the dLNs after TheraVac plus cGAMP therapy, the dLNs of mice harboring melanoma tumors with or without treatment were harvested to make single-cell suspensions for immune staining and flow cytometric analysis. TheraVac plus cGAMP treatment resulted in a marked increase in the frequency of effector/memory CD4 and CD8 T cells in the dLNs (Fig. 5A–C). The central memory ($CD62L^+/CD44^+$) CD4, CD8 T cells were also greatly enhanced (Fig. 5A–C).

The efficient induction of CTLs specific for autologous tumors is a critical role for adaptive tumor immunity (33). To determine whether functional antimelanoma CTLs were induced by treatment with TheraVac plus cGAMP, dLNs cells were cocultured with melanoma cells ex vivo for 18 h and the resultant CD8 cells were analyzed for the expression of CD107a. As shown by (Fig. 5D–F), the frequency levels of $CD8^+CD107a^+$ T cells in the dLNs were markedly increased by TheraVac treatment, which was further significantly elevated by TheraVac plus cGAMP treatment. Therefore, TheraVac plus cGAMP treatment of melanoma-bearing mice promoted generation of effector/memory CD4, CD8 T and central memory CD4, CD8 T cells and melanoma-specific functional CTLs in the dLNs, a profile characteristic of antitumor immunity.

Discussion

Melanoma, a multidrug-resistant tumor, is difficult to eliminate in mouse models, and until now this could not be achieved by either single or combination therapies or adoptive transfer of large numbers of T cells (34). Although TheraVac, consisting of N1, R848, and anti-PDL-1, could effectively cure mouse liver (Hepa1-6) (35), colon (CT26), thymoma (EG7), lung (LLC), and kidney (RENCA) tumors (36), it only slowed melanoma tumor growth transiently. In this study, we have shown that TheraVac plus cGAMP combination therapy effectively stimulated an endogenous immune response to overcome the resistance of melanin-producing mouse melanomas. This combination therapy not only caused complete regression of melanomas but it also resulted in the acquisition of specific protective immunity against the treated tumors.

How does the combination of TheraVac and cGAMP become a curative therapy for the drug-resistant melanin-producing mouse melanomas? This could be achieved based on at least two mechanistic modes of action that work collaboratively. First, the synergistic effect of cGAMP and the immunostimulatory arms of TheraVac on the maturation of DCs (Fig. 1) indicate that when administered together into the tumors, cGAMP would promote more potent maturation and activation of TiDCs present in these melanoma tumors. The more potent maturation and activation of TiDCs would cause more TiDCs trafficking to dLNs to trigger the generation of more melanoma-specific T cells that subsequently migrate to the tumor tissue for the elimination of melanoma cells. In accordance with this scenario, M3 melanoma-bearing mice treated with TheraVac plus cGAMP compared with mice treated with TheraVac alone showed 1) higher levels of central/memory CD4, CD8 T and effector/memory CD4, CD8 T cells in the dLNs (Fig. 5B, 5C), 2) higher levels of functional melanoma-specific CD8 CTLs in the dLNs (Fig. 5D–F), 3) more effector/memory CD4 T and CD8 T cells in the tumor tissue (Fig. 4E, 4F), and 4) a more robust Th1 signature in the treated tumors as evidenced by the elevated levels of IFN-γ and Th1 effector-recruiting chemokines such as CXCL9 and CXCL10 in the tumor tissue (Fig. 4D). It has also recently been reported that direct delivery of STING agonists to tumors promotes TiDC activation and generation of antitumor immunity (31, 37, 38). Inclusion of the checkpoint inhibitor anti-PDL-1 in the therapeutic regimen would allow effector/memory T cells to function longer by preventing silencing/exhaustion (15). Thus, this combination of TheraVac and cGAMP is more therapeutically potent than TheraVac alone on mouse melanomas.

The second mechanistic mode of action presumably relies on the capacity of cGAMP to trigger the activation of STING signaling pathway in melanoma tissue for elevating the production of type I IFNs. It is well established that type I INFs produced as a result of STING activation are responsible for reprogramming the TME from an immunosuppressive M2 to an immunoprotective M1 status (31, 38–41), activating NK cells (37) and promoting the recruitment of immune cells (30). Additionally, elevated production of type I IFNs is likely to inhibit melanoma growth given the direct antiproliferative effect of IFNs on melanoma cells in vitro and in vivo (42, 43). Because both N1 (Supplemental Fig. 2) and R848 (32, 44) also have the capacity to trigger M1 macrophage polarization and activation, the combination of cGAMP, N1, and R848 would greatly enhance M1 macrophage polarization/activation in melanoma tumors. Indeed, M3 melanoma-bearing mice treated with TheraVac plus cGAMP compared with mice treated with TheraVac alone exhibited higher levels of IFN-β expression (Fig. 4D) as well as macrophage accumulation (Fig. 4C) in melanoma tissues. Together with the previous report showing that TheraVac was shown to reduce the level of intratumoral regulatory T cells (36), TheraVac plus cGAMP combinational therapy would, by cooperatively stimulating production of type I IFNs, markedly reduce the immunosuppression of the melanoma TME, promote M1 macrophage and NK cell activation, and inhibit the proliferation of melanoma cells. The synergistically enhanced innate and adaptive antimelanoma immune responses triggered by treatment with TheraVac plus cGAMP presumably work in concert for the immunologic elimination of cancer cells, resulting in curative therapy of melanin-producing melanomas.

Our data show that Th1-type chemokines CXCL9, CXCL10, and IFN-γ are strongly induced by TheraVac plus cGAMP treatment. This is consistent with previous studies, which reported that CXCL9 and CXCL10 and IFN-γ upregulation is indicative of Th1 antitumor immunity that correlates with the effectiveness of antitumor immunotherapy (45, 46). This also suggests that both $CD4^+$ and $CD8^+$ T cells are probably needed to exert the therapeutic effects of TheraVac plus cGAMP. Many reports have recently suggested the important roles of the adaptive immune system, such as $CD8^+$ T cell responses to tumors (47, 48). cGAMP in our vaccination regimens might also contribute to the maintenance of $CD8^+$ T cell stemness for the promotion of antitumor T cell therapy (17, 49).

It is noteworthy that no clear side effect was observed in mice with the TheraVac plus cGAMP treatment. Mice harboring melanoma tumors cured with TheraVac plus cGAMP did not experience significant loss of body weight or patchy hair loss (data not shown), indicating the lack of undesirable side effects such as autoimmune responses. Additionally, TheraVac plus cGAMP achieves successful tumor vaccination without relying on the use of exogenous tumor-associated Ags, and therefore it can potentially be used for the treatment of many other cancers.

In summary, our immunotherapeutic regimen, a combination of TheraVac and cGAMP, can induce the generation of robust antimelanoma immune responses to cure mice with melanin-producing melanomas. The curative effect of this is based on coordinated promotion of the activation/generation of both innate (DCs and

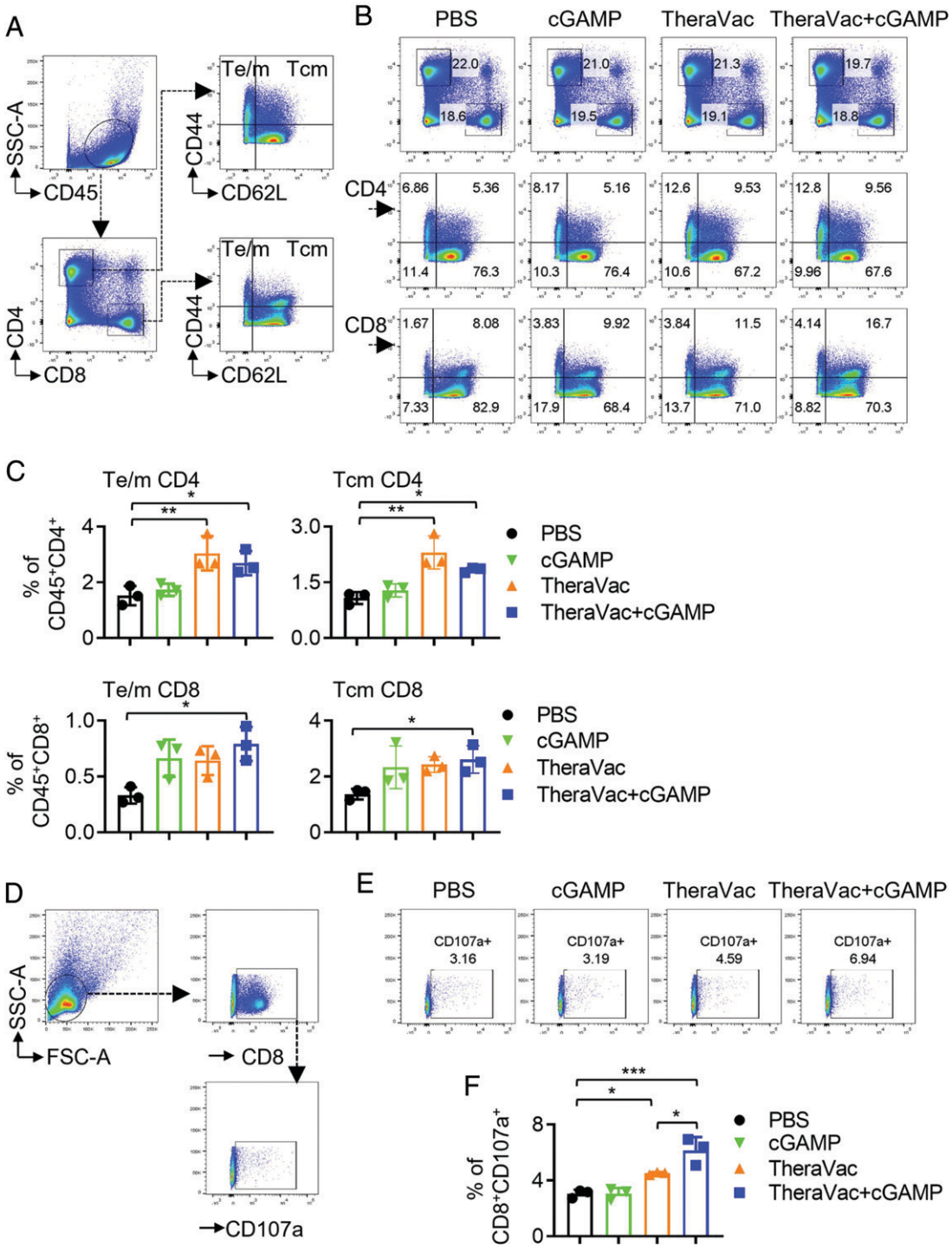

FIGURE 5. Immunoprofiling of tumor-draining lymph nodes of M3-bearing mice treated with TheraVac and cGAMP alone or in combination. C57BL/6 mice inoculated s.c. with M3 melanoma cells (2×10^5/mouse) into the flank were treated on days 13, 16, and 20 with PBS, cGAMP (5 μg/injection), TheraVac (10 μg of each component/injection), or TheraVac plus cGAMP. Forty-eight hours after the last treatment, mice were euthanized to remove the draining inguinal lymph nodes for the preparation of single-cell suspensions for flow cytometry analysis of T cell activation. (**A**) Gating strategy. (**B**) Plot of tumor of one mouse. (**C**) Average (mean ± SD; $n = 5$) of individual mouse of each group. $CD44^{high}/CD62L^{-}$ of $CD4^{+}$ and $CD8^{+}$ T cells were considered as effector/memory T (Te/m) cells whereas $CD44^{+}/CD62L^{+}$ of $CD4^{+}$ and $CD8^{+}$ cells were identified as central memory T (Tcm) cells. (**D**) Gating strategy. (**E**) Plot of the dLNs of one mouse. (**F**) Average (mean ± SD; $n = 3$) of individual mouse of each group. $CD107a^{+}CD8^{+}$ T cells were identified as M3-specific CTLs. Shown are the results of one experiment representative of two. $*p < 0.05$, $**p < 0.01$, $***p < 0.001$, between the sham and treated group using one-way ANOVA followed by a Tukey's post hoc test.

M1 macrophages) and melanoma-specific effector and memory CD4 and CD8 T cells as well as conversion of the immunosuppressive TME into an immunogenic TME. It will be interesting to further investigate whether this combination can be applicable for treatment of melanomas in humans.

Acknowledgments

We are grateful to Dr. Glenn Merlino and the colleagues of his laboratory for providing the melanoma cell lines. We thank Jocelyn Bassler and Yanyu Wang (CSL, CSP, Leidos Biomedical Research, Inc.) for Meso Scale Discovery cytokine assays, and Debra Tross, Anna Trivett, and Jessica Neder

(LCIM, CCR, NCI–Frederick, National Institutes of Health) for administrative support.

Disclosures

The authors have no financial conflicts of interest.

References

1. Gray-Schopfer, V., C. Wellbrock, and R. Marais. 2007. Melanoma biology and new targeted therapy. *Nature* 445: 851–857.
2. Akbani, R., K. C. Akdemir, B. A. Aksoy, M. Albert, A. Ally, S. B. Amin, H. Arachchi, A. Arora, J. T. Auman, B. Ayala, et al.; Cancer Genome Atlas Network. 2015. Genomic classification of cutaneous melanoma. *Cell* 161: 1681–1696.
3. Maertens, O., R. Kuzmickas, H. E. Manchester, C. E. Emerson, A. G. Gavin, C. J. Guild, T. C. Wong, T. De Raedt, C. Bowman-Colin, E. Hatchi, et al. 2019. MAPK pathway suppression unmasks latent DNA repair defects and confers a chemical synthetic vulnerability in *BRAF-, NRAS-*, and *NF1*-mutant melanomas. *Cancer Discov.* 9: 526–545.
4. Sanchez-Laorden, B., A. Viros, M. R. Girotti, M. Pedersen, G. Saturno, A. Zambon, D. Niculescu-Duvaz, S. Turajlic, A. Hayes, M. Gore, et al. 2014. BRAF inhibitors induce metastasis in RAS mutant or inhibitor-resistant melanoma cells by reactivating MEK and ERK signaling. *Sci. Signal.* 7: ra30.
5. Ribas, A., D. Lawrence, V. Atkinson, S. Agarwal, W. H. Miller, Jr., M. S. Carlino, R. Fisher, G. V. Long, F. S. Hodi, J. Tsoi, et al. 2019. Combined BRAF and MEK inhibition with PD-1 blockade immunotherapy in BRAF-mutant melanoma. [Published erratum appears in 2019 *Nat. Med.* 25: 1319.] *Nat. Med.* 25: 936–940.
6. Domingues, B., J. M. Lopes, P. Soares, and H. Pópulo. 2018. Melanoma treatment in review. *ImmunoTargets Ther.* 7: 35–49.
7. Rosenberg, S. A., J. C. Yang, and N. P. Restifo. 2004. Cancer immunotherapy: moving beyond current vaccines. *Nat. Med.* 10: 909–915.
8. Hodi, F. S., S. J. O'Day, D. F. McDermott, R. W. Weber, J. A. Sosman, J. B. Haanen, R. Gonzalez, C. Robert, D. Schadendorf, J. C. Hassel, et al. 2010. Improved survival with ipilimumab in patients with metastatic melanoma. *N. Engl. J. Med.* 363: 711–723.
9. Hu, M., M. Zhou, X. Bao, D. Pan, M. Jiao, X. Liu, F. Li, and C. Y. Li. 2021. ATM inhibition enhances cancer immunotherapy by promoting mtDNA leakage and cGAS/STING activation. *J. Clin. Invest.* 131: e139333.
10. Rotte, A. 2019. Combination of CTLA-4 and PD-1 blockers for treatment of cancer. *J. Exp. Clin. Cancer Res.* 38: 255.
11. Seidel, J. A., A. Otsuka, and K. Kabashima. 2018. Anti-PD-1 and anti-CTLA-4 therapies in cancer: mechanisms of action, efficacy, and limitations. *Front. Oncol.* 8: 86.
12. Chae, Y. K., A. Arya, W. Iams, M. R. Cruz, S. Chandra, J. Choi, and F. Giles. 2018. Current landscape and future of dual anti-CTLA4 and PD-1/PD-L1 blockade immunotherapy in cancer; lessons learned from clinical trials with melanoma and non-small cell lung cancer (NSCLC). *J. Immunother. Cancer* 6: 39.
13. Alam, M. M., D. Yang, A. Trivett, T. J. Meyer, and J. J. Oppenheim. 2018. HMGN1 and R848 synergistically activate dendritic cells using multiple signaling pathways. *Front. Immunol.* 9: 2982.
14. Yang, D., Z. Han, M. M. Alam, and J. J. Oppenheim. 2018. High-mobility group nucleosome binding domain 1 (HMGN1) functions as a Th1-polarizing alarmin. *Semin. Immunol.* 38: 49–53.
15. Nie, Y. J., D. Yang, A. Trivett, Z. Han, H. Y. Xin, X. Chen, and J. J. Oppenheim. 2017. Development of a curative therapeutic vaccine (TheraVac) for the treatment of large established tumors. *Sci. Rep.* 7: 14186.
16. He, Y., C. Hong, E. Z. Yan, S. J. Fletcher, G. Zhu, M. Yang, Y. Li, X. Sun, D. J. Irvine, J. Li, and P. T. Hammond. 2020. Self-assembled cGAMP-STINGΔTM signaling complex as a bioinspired platform for cGAMP delivery. *Sci. Adv.* 6: eaba7589.
17. Li, W., L. Lu, J. Lu, X. Wang, C. Yang, J. Jin, L. Wu, X. Hong, F. Li, D. Cao, et al. 2020. cGAS-STING-mediated DNA sensing maintains $CD8^+$ T cell stemness and promotes antitumor T cell therapy. *Sci. Transl. Med.* 12: eaay9013.
18. Melnikova, V. O., S. V. Bolshakov, C. Walker, and H. N. Ananthaswamy. 2004. Genomic alterations in spontaneous and carcinogen-induced murine melanoma cell lines. *Oncogene* 23: 2347–2356.
19. Overwijk, W. W., and N. P. Restifo. 2001. B16 as a mouse model for human melanoma. *Curr. Protoc. Immunol.* Chapter 20:Unit 20.1.
20. Nakamura, K., N. Yoshikawa, Y. Yamaguchi, S. Kagota, K. Shinozuka, and M. Kunitomo. 2002. Characterization of mouse melanoma cell lines by their mortal malignancy using an experimental metastatic model. *Life Sci.* 70: 791–798.
21. Pérez-Guijarro, E., H. H. Yang, R. E. Araya, R. El Meskini, H. T. Michael, S. K. Vodnala, K. L. Marie, C. Smith, S. Chin, K. C. Lam, et al. 2020. Multimodel preclinical platform predicts clinical response of melanoma to immunotherapy. [Published erratum appears in 2021 *Nat. Med.* 27: 355.] *Nat. Med.* 26: 781–791.
22. Yang, D., Q. Chen, H. Yang, K. J. Tracey, M. Bustin, and J. J. Oppenheim. 2007. High mobility group box-1 protein induces the migration and activation of human dendritic cells and acts as an alarmin. *J. Leukoc. Biol.* 81: 59–66.
23. De Yang, Q., A. P. Chen, G. M. Schmidt, J. M. Anderson, J. Wang, J. J. Wooters, Oppenheim, and O. Chertov. 2000. LL-37, the neutrophil granule- and epithelial cell-derived cathelicidin, utilizes formyl peptide receptor-like 1 (FPRL1) as a receptor to chemoattract human peripheral blood neutrophils, monocytes, and T cells. *J. Exp. Med.* 192: 1069–1074.
24. Inaba, K., M. Pack, M. Inaba, H. Sakuta, F. Isdell, and R. M. Steinman. 1997. High levels of a major histocompatibility complex II-self peptide complex on dendritic cells from the T cell areas of lymph nodes. *J. Exp. Med.* 186: 665–672.
25. Yang, D., Q. Chen, S. B. Su, P. Zhang, K. Kurosaka, R. R. Caspi, S. M. Michalek, H. F. Rosenberg, N. Zhang, and J. J. Oppenheim. 2008. Eosinophil-derived neurotoxin acts as an alarmin to activate the TLR2-MyD88 signal pathway in dendritic cells and enhances Th2 immune responses. *J. Exp. Med.* 205: 79–90.
26. Han, Z., S. Liu, H. Lin, A. L. Trivett, S. Hannifin, D. Yang, and J. J. Oppenheim. 2019. Inhibition of murine hepatoma tumor growth by cryptotanshinone involves TLR7-dependent activation of macrophages and induction of adaptive antitumor immune defenses. *Cancer Immunol. Immunother.* 68: 1073–1085.
27. Woo, S. R., M. B. Fuertes, L. Corrales, S. Spranger, M. J. Furdyna, M. Y. Leung, R. Duggan, Y. Wang, G. N. Barber, K. A. Fitzgerald, et al. 2014. STING-dependent cytosolic DNA sensing mediates innate immune recognition of immunogenic tumors. [Published erratum appears in 2015 *Immunity* 42: 199.] *Immunity* 41: 830–842.
28. Yum, S., M. Li, Y. Fang, and Z. J. Chen. 2021. TBK1 recruitment to STING activates both IRF3 and NF-κB that mediate immune defense against tumors and viral infections. *Proc. Natl. Acad. Sci. USA* 118: e2100225118.
29. Clark, K., L. Plater, M. Peggie, and P. Cohen. 2009. Use of the pharmacological inhibitor BX795 to study the regulation and physiological roles of TBK1 and IκB kinase ε: a distinct upstream kinase mediates Ser-172 phosphorylation and activation. *J. Biol. Chem.* 284: 14136–14146.
30. Weiss, J. M., M. V. Guérin, F. Regnier, G. Renault, I. Galy-Fauroux, L. Vimeux, V. Feuillet, E. Peranzoni, M. Thoreau, A. Trautmann, and N. Bercovici. 2017. The STING agonist DMXAA triggers a cooperation between T lymphocytes and myeloid cells that leads to tumor regression. *OncoImmunology* 6: e1346765.
31. Jing, W., D. McAllister, E. P. Vonderhaar, K. Palen, M. J. Riese, J. Gershan, B. D. Johnson, and M. B. Dwinell. 2019. STING agonist inflames the pancreatic cancer immune microenvironment and reduces tumor burden in mouse models. *J. Immunother. Cancer* 7: 115.
32. Liu, Z., Y. Xie, Y. Xiong, S. Liu, C. Qiu, Z. Zhu, H. Mao, M. Yu, and X. Wang. 2020. TLR 7/8 agonist reverses oxaliplatin resistance in colorectal cancer via directing the myeloid-derived suppressor cells to tumoricidal M1-macrophages. *Cancer Lett.* 469: 173–185.
33. Durgeau, A., Y. Virk, S. Corgnac, and F. Mami-Chouaib. 2018. Recent advances in targeting CD8 T-cell immunity for more effective cancer immunotherapy. *Front. Immunol.* 9: 14.
34. Moynihan, K. D., C. F. Opel, G. L. Szeto, A. Tzeng, E. F. Zhu, J. M. Engreitz, R. T. Williams, K. Rakhra, M. H. Zhang, A. M. Rothschilds, et al. 2016. Eradication of large established tumors in mice by combination immunotherapy that engages innate and adaptive immune responses. *Nat. Med.* 22: 1402–1410.
35. Han, Z., D. Yang, A. Trivett, and J. J. Oppenheim. 2017. Therapeutic vaccine to cure large mouse hepatocellular carcinomas. *Oncotarget* 8: 52061–52071.
36. Nie, Y., D. Yang, A. Trivett, Z. Han, H. Xin, X. Chen, and J. J. Oppenheim. 2017. Development of a curative therapeutic vaccine (TheraVac) for the treatment of large established tumors. *Sci. Rep.* 7: 14186.
37. Fu, J., D. B. Kanne, M. Leong, L. H. Glickman, S. M. McWhirter, E. Lemmens, K. Mechette, J. J. Leong, P. Lauer, W. Liu, et al. 2015. STING agonist formulated cancer vaccines can cure established tumors resistant to PD-1 blockade. *Sci. Transl. Med.* 7: 283ra52.
38. Corrales, L., L. H. Glickman, S. M. McWhirter, D. B. Kanne, K. E. Sivick, G. E. Katibah, S. R. Woo, E. Lemmens, T. Banda, J. J. Leong, et al. 2015. Direct activation of STING in the tumor microenvironment leads to potent and systemic tumor regression and immunity. *Cell Rep.* 11: 1018–1030.
39. Downey, C. M., M. Aghaei, R. A. Schwendener, and F. R. Jirik. 2014. DMXAA causes tumor site-specific vascular disruption in murine non-small cell lung cancer, and like the endogenous non-canonical cyclic dinucleotide STING agonist, 2′3′-cGAMP, induces M2 macrophage repolarization. *PLoS One* 9: e99988.
40. Lam, K. C., R. E. Araya, A. Huang, Q. Chen, M. Di Modica, R. R. Rodrigues, A. Lopès, S. B. Johnson, B. Schwarz, E. Bohrnsen, et al. 2021. Microbiota triggers STING-type I IFN-dependent monocyte reprogramming of the tumor microenvironment. *Cell* 184: 5338–5356.e21.
41. Lee, S. J., H. Yang, W. R. Kim, Y. S. Lee, W. S. Lee, S. J. Kong, H. J. Lee, J. H. Kim, J. Cheon, B. Kang, et al. 2021. STING activation normalizes the intraperitoneal vascular-immune microenvironment and suppresses peritoneal carcinomatosis of colon cancer. *J. Immunother. Cancer* 9: e002195.
42. Nakayama, J., K. Toyofuku, A. Urabe, S. Taniguchi, and Y. Hori. 1993. A combined therapeutic modality with hyperthermia and locally administered rIFN-β inhibited the growth of B16 melanoma in association with the modulation of cellular infiltrates. *J. Dermatol. Sci.* 6: 240–246.
43. Merkel, C. A., R. F. Medrano, V. G. Barauna, and B. E. Strauss. 2013. Combined p19Arf and interferon-beta gene transfer enhances cell death of B16 melanoma in vitro and in vivo. *Cancer Gene Ther.* 20: 317–325.
44. Rodell, C. B., S. P. Arlauckas, M. F. Cuccarese, C. S. Garris, R. Li, M. S. Ahmed, R. H. Kohler, M. J. Pittet, and R. Weissleder. 2018. TLR7/8-agonist-loaded nanoparticles promote the polarization of tumour-associated macrophages to enhance cancer immunotherapy. *Nat. Biomed. Eng.* 2: 578–588.
45. Liu, S., Z. Han, A. L. Trivett, H. Lin, S. Hannifin, D. Yang, and J. J. Oppenheim. 2019. Cryptotanshinone has curative dual anti-proliferative and immunotherapeutic effects on mouse Lewis lung carcinoma. *Cancer Immunol. Immunother.* 68: 1059–1071.
46. Wang, H., S. Li, Q. Wang, Z. Jin, W. Shao, Y. Gao, L. Li, K. Lin, L. Zhu, H. Wang, et al. 2021. Tumor immunological phenotype signature-based high-throughput screening for the discovery of combination immunotherapy compounds. *Sci. Adv.* 7: eabd7851.
47. Kvistborg, P., D. Philips, S. Kelderman, L. Hageman, C. Ottensmeier, D. Joseph-Pietras, M. J. Welters, S. van der Burg, E. Kapiteijn, O. Michielin, et al. 2014. Anti-CTLA-4 therapy broadens the melanoma-reactive $CD8^+$ T cell response. *Sci. Transl. Med.* 6: 254ra128.
48. Krishna, S., F. J. Lowery, A. R. Copeland, E. Bahadiroglu, R. Mukherjee, L. Jia, J. T. Anibal, A. Sachs, S. O. Adebola, D. Gurusamy, et al. 2020. Stem-like CD8 T cells mediate response of adoptive cell immunotherapy against human cancer. *Science* 370: 1328–1334.
49. Sivick, K. E., A. L. Desbien, L. H. Glickman, G. L. Reiner, L. Corrales, N. H. Surh, T. E. Hudson, U. T. Vu, B. J. Francica, T. Banda, et al. 2018. Magnitude of therapeutic STING activation determines $CD8^+$ T cell-mediated anti-tumor immunity. [Published erratum appears in 2019 *Cell Rep.* 29: 785–789.] *Cell Rep.* 25: 3074–3085.e5.